

# LLRF CONTROL OF HIGH $Q_L$ CAVITIES FOR THE LCLS-II \*

L. R. Doolittle, G. Huang, A. Ratti, C. Serrano<sup>†</sup>, LBNL, Berkeley, California, USA  
 B. E. Chase, E. W. Cullerton, J. A. Einstein, Fermilab, Batavia, Illinois, USA  
 R. Bachimanchi, C. Hovater, JLab, Newport News, Virginia, USA  
 S. Babel, M. Boyes, B. Hong, SLAC, Menlo Park, California, USA

## Abstract

The SLAC National Accelerator Laboratory is planning an upgrade (LCLS-II) to the Linear Coherent Light Source (SCRf) linac. The nature of the machine places stringent requirements in the Low-Level RF (LLRF) system, expected to control the cavity fields within  $0.01^\circ$  in phase and 0.01% in amplitude, which is equivalent to a longitudinal motion of the cavity structure in the nanometer range. This stability has been achieved in the past but never for hundreds of superconducting cavities in Continuous-Wave (CW) operation. The difficulty resides in providing the ability to reject disturbances from the cryomodule, which is incompletely known as it depends on the cryomodule structure itself (currently under development at JLab and Fermilab) and the harsh accelerator environment. Previous experience in the field and an extrapolation to the cavity design parameters (relatively high  $Q_L \approx 4 \times 10^7$ , implying a half-bandwidth of around 16 Hz) suggest the use of strong RF feedback to reject the projected noise disturbances, which in turn demands careful engineering of the entire system. The project has passed the conceptual design phase and is approaching the final design phase. LLRF prototypes are currently under construction and expected to be exercised in a cryomodule test stand at both JLab and Fermilab (using the LCLS-II TESLA-ILC type 1.3 GHz cavities) before the end of 2016 to validate the engineering design presented here.

## INTRODUCTION

LCLS-II [1] adds a 4 GeV L-band (1.3 GHz) superconducting linac to the first 700 meters of the SLAC tunnel, increasing the repetition rate of LCLS from 120 Hz to 1 MHz (operating in CW) and an average beam current of  $100 \mu\text{A}$ . The SCRf linac includes 35 ILC-style cryomodules (eight 9-cell cavities each) for a total of 280 cavities. LCLS-II will become the world's first X-ray Free Electron Laser (FEL) providing CW pulses, probing the motion of molecules, atoms and electrons on their natural time scales (femtoseconds and faster) enabling a broad range of new energy science.

Accelerating cavity RF field stability affects the final FEL performance through its relationship with the longitudinal beam dynamics, namely on final beam energy, peak current and arrival time [2]. Energy stability in the order of  $10^{-5}$  converts to different RF stability requirements in each Linac section;  $0.01^\circ$  in phase and 0.01% in amplitude represents

\* This work was supported by the LCLS-II Project and the U.S. Department of Energy, Contract DE-AC02-76SF00515

<sup>†</sup> CSerrano@lbl.gov

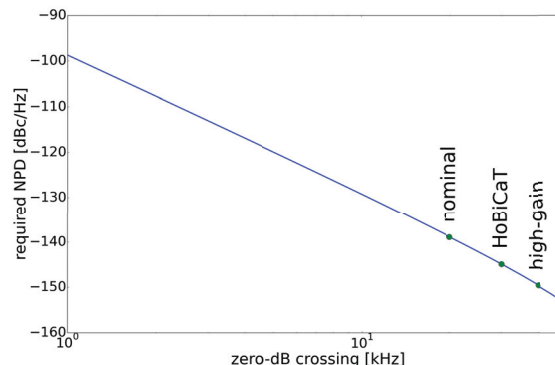


Figure 1: Noise requirements vs. zero-dB crossing.

the tightest requirement, and that for which the LLRF system is engineered.

The baseline LCLS-II project does not include fast beam-based feedback, thus the RF stability requirement has to be satisfied by the LLRF system alone for noise integrated above 1 Hz, with beam currents up to  $100 \mu\text{A}$  and a bunch repetition rate of up to 1 MHz. Enough RF power is made available by the 3.8 kW SSAs to operate the cavities at a nominal 16 MV/m, with RF budget allocated to beam loading and RF corrections (including  $\pm 10$  Hz peak cavity detuning due to microphonics).

The LLRF system design [3] is centered around a Precision Receiver Chassis (PRC) providing low-noise detection of the cavity probe signal, an RF Station (RFS) chassis implementing digital RF control in an FPGA, and two other chassis dedicated to cavity resonance control (driving fast piezos and slow stepper motors) and interlocks.

## FIELD CONTROL CONSIDERATIONS

The very narrow bandwidth of the cavity makes it very sensitive to microphonics, where nanometers of mechanical deformation translates into tens of Hz of detuning. The nature of the disturbance (external noise sources, mechanical resonances, couplings, etc.) depends on the cryomodule structure itself and the accelerator environment, which are both imperfectly known at this stage of the design. Microphonics rejection typically requires a control bandwidth in the tens of kHz range, where the optimal controller settings will be measured in the accelerator environment. The combination of high sensitivity to microphonics and the tight field stability requirements makes it necessary for the LLRF design to support high feedback gain.

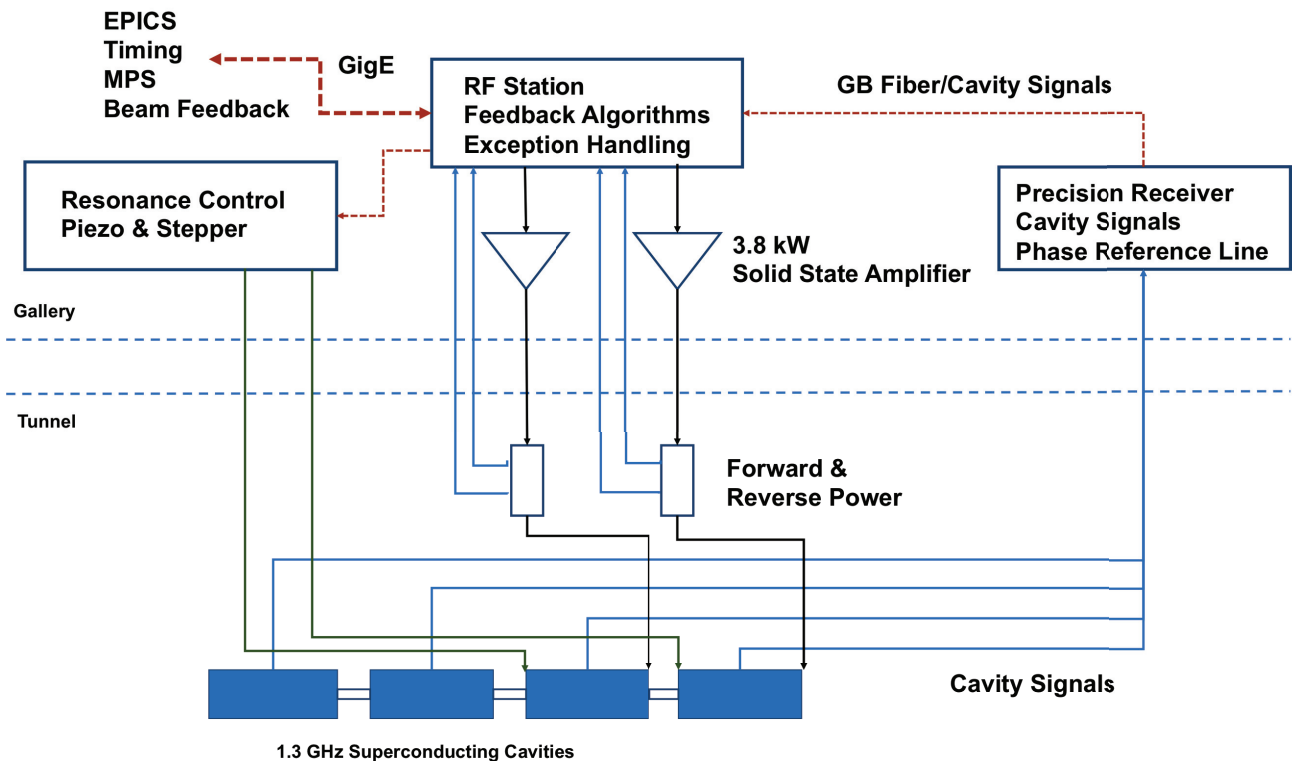


Figure 2: Block diagram of the LCLS-II LLRF design, including controls for two 1.3-GHz superconducting cavities.

The above considerations form the basis for the engineering of the LLRF system and present different trade-offs. Increasing the open-loop zero-dB crossing helps rejecting cavity disturbances, but (as an example) achieving a 20 kHz open-loop zero-dB crossing with a 16 Hz cavity bandwidth implies a proportional gain of about 1200. Any noise in the cavity field measurement chain will get amplified by the same factor and the amplified noise signal will be transferred directly into the input of the SSA. This places the critical point of the design in building a quiet sensor for the cavity field. Figure 1 shows the relationship between the noise tolerance in the cavity field detection (down-conversion, digitizing, etc.) in units of dBc/Hz and the choice of open-loop zero-dB crossing (and therefore proportional gain). The assumption is a 4% RMS (amplitude) allowed SSA drive noise, 1  $\mu$ s hardware delay, 16 Hz cavity bandwidth, and 1/12T stability guideline.

## SYSTEM ENGINEERING DESIGN

In order to build a quiet sensor, the cavity probe signals are downconverted and digitized in a separate, temperature-stabilized chassis (the Precision Receiver Chassis, PRC) described in detail later. The PRC has an FPGA board that acquires the digitized cavity signals and sends them over a digital optical-fiber link to the RF Station, implementing the feedback algorithm. Figure 2 shows a block diagram of the LLRF design where 4 out of the 8 cavities in a cryomodule are represented along with the controls for two cavities through one penetration. Note the physical separation of the forward and reflected signals from the cavity probe, responding to the engineering needs discussed above.

ration of the forward and reflected signals from the cavity probe, responding to the engineering needs discussed above.

## PROTOTYPE CHARACTERIZATION

Prototypes for all the components in the LCLS-II LLRF system [3] have been built and tests with the LCLS-II cryomodules are expected before the end of 2016. Figure 3 shows a block diagram of the characterization exercise for the up and downconverters (designed at Fermilab) and the digitizer boards (designed at LBNL). The FPGA board is the common platform used in the RF stations, precision receivers, interlocks and resonance control chassis illustrated in Figure 2.

A 1320 MHz local oscillator provides a frequency reference as in the production system. A 203/264 (non-binary) NCO drives the DAC in the digitizer board at a 188.6 MHz clock (derived from the 1320 MHz LO with a divide-by-7). This produces 145 MHz, which is mixed up to 1300 MHz and then back down to 20 MHz (the Intermediate Frequency, IF). The ADCs receives 20 MHz with a clock of 94.3 MHz (derived using a divide-by-14 output of the same divider chip). Note that  $20 \text{ MHz} = 7/33 \cdot \text{the ADC clock}$ .

The use of two independent ADC channels allows for computing correlations and separating the noise contributions from the DAC + upconverter chain from the downconverter + ADC chain as shown in Figure 3 [4]. If we call the ADC signals  $x$  and  $y$  respectively, and we convert the time-series signals to frequency domain, we can compute the autocor-

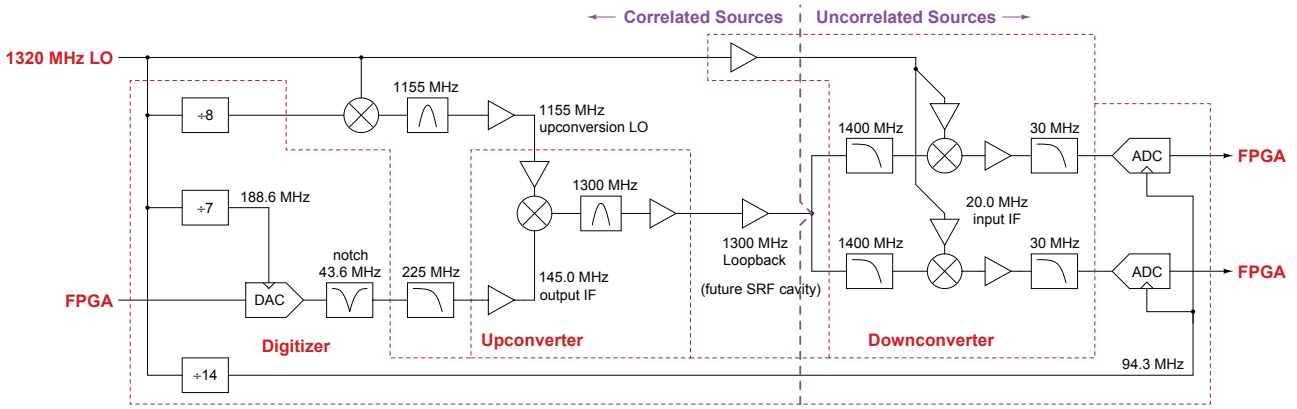


Figure 3: Test configuration to evaluate LLRF analog hardware performance.

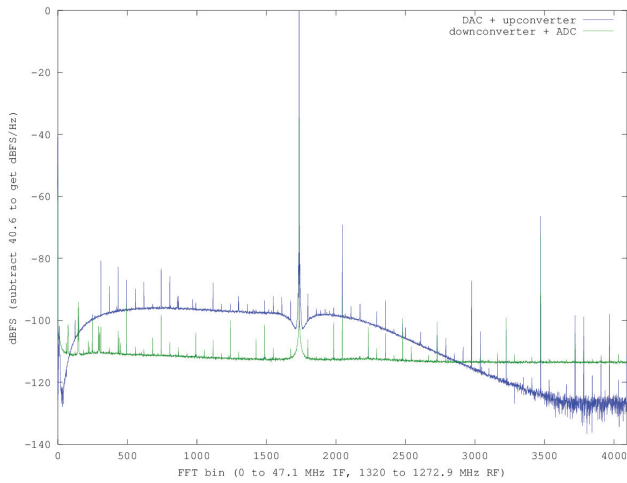


Figure 4: Power spectra of the noise contributions.

relation for each channel we get power spectra for the two channels:

$$S_{xx} = \langle FFT(x) \cdot FFT(y)^* \rangle$$

$$S_{yy} = \langle FFT(y) \cdot FFT(x)^* \rangle$$

Calculating the cross-correlation of the two channels we obtain the noise power of the added noise by the DAC + upconverter chain:

$$S_{yx} = \langle FFT(y) \cdot FFT(x)^* \rangle \quad (1)$$

and we can then deduce the contribution of the downconverter + ADC chain by:

$$Diff = S_{xx} + S_{yy} - 2 \cdot |S_{yx}| \quad (2)$$

The critical receiver channel noise power density (including ADC) is seen to reach the desired -150 dBc/Hz as required for stiff cavity feedback (see Figure 4). Spurs are small (generally less than 100 dBc) and have well-defined frequencies based purely on divider ratios.

Close-in noise spectra have also been measured, showing clean  $1/f$  noise properties in both the ADC and RF gear.

By adding attenuators to the 1300 MHz signal, it has been confirmed that the unusual split-LO design achieves its goal of providing strong isolation between the transmit channel and the receive channels. The measured isolation exceeds 100 dB.

Since all the filters used in the above experiment are relatively wide-band, the close-in phase noise of the LO fully cancels out. When driving an SRF cavity, of course that condition is no longer satisfied, and a low-phase-noise LO will therefore be required to achieve stiff feedback.

## CONCLUSIONS

The LCLS-II LLRF system is approaching the final design phase. The challenging task of controlling high  $Q_L$  cavities for the LCLS-II superconducting linac has properly analyzed and simulated [5] identifying the need for high gain feedback. With the conclusions of the analysis the LLRF system has been carefully engineered and the results obtained with the prototype hardware show promising results.

## REFERENCES

- [1] J. N. Galayda, "The new LCLS-II project: status and challenges," in *Proc. LINAC'14*, Geneva, Switzerland, August 2014, paper TU10A04, pp. 404–408.
- [2] P. Emma, "LCLS-II Physics Requirement Document: Linac Requirements," LCLSII-2.4-PR-0041-R4, Feb. 2016.
- [3] L. R. Doolittle *et al.*, "The LCLS-II LLRF system," in *Proc. IPAC'15*, Richmond, VA, USA, May 2015, paper MOPWI021, pp. 1195–1197.
- [4] E. Rubiola, "Phase noise and frequency stability in oscillators," Cambridge University Press, 2010, ISBN 052115328X.
- [5] C. Serrano *et al.*, "End-to-end FEL beam stability simulation engine," in *Proc. IPAC'16*, Busan, South Korea, May 2016, paper WEPOR043.